The mouse mutation "thrombocytopenia and cardiomyopathy" *(trac)* disrupts *Abcg5*: a spontaneous single gene model for human hereditary phytosterolemia/sitosterolemia

Thomas H. Chase,[1] Bonnie L. Lyons,[1] Roderick T. Bronson,[1] Oded Foreman,[1] Leah Rae Donahue,[1] Lisa M. Burzenski,[1] Bruce Gott,[1] Priscilla Lane,[1] Belinda Harris,[1] Uta Ceglarek,[2] Joachim Thiery,[2] Henning Wittenburg,[2] Jonathan N. Thon,[3] Joseph E. Italiano Jr,[3] Kenneth R. Johnson,[1] and Leonard D. Shultz[1]

[1]The Jackson Laboratory, Bar Harbor, ME; [2]Universität Leipzig, Leipzig, Germany; and [3]Brigham and Women's Hospital, Children's Hospital Boston, and Harvard Medical School, Boston, MA

The spontaneous mouse mutation "thrombocytopenia and cardiomyopathy" *(trac)* causes macrothrombocytopenia, prolonged bleeding times, anemia, leukopenia, infertility, cardiomyopathy, and shortened life span. Homozygotes show a 20-fold decrease in platelet numbers and a 3-fold increase in platelet size with structural alterations and functional impairments in activation and aggregation. Megakaryocytes in *trac/trac* mice are present in increased numbers, have poorly developed demarcation membrane systems, and have decreased polyploidy. The thrombocytopenia is not intrinsic to defects at the level of hematopoietic progenitor cells but is associated with a microenvironmental abnormality. The *trac* mutation maps to mouse chromosome 17, syntenic with human chromosome 2p21-22. A G to A mutation in exon 10 of the adenosine triphosphate (ATP)–binding cassette subfamily G, member 5 *(Abcg5)* gene, alters a tryptophan codon (UGG) to a premature stop codon (UAG). Crosses with mice doubly transgenic for the human *ABCG5* and *ABCG8* genes rescued platelet counts and volumes. ABCG5 and ABCG8 form a functional complex that limits dietary phytosterol accumulation. Phytosterolemia in *trac/trac* mice confirmed a functional defect in the ABCG5/ABCG8 transport system. The *trac* mutation provides a new clinically significant animal model for human phytosterolemia and provides a new means for studying the role of phytosterols in hematologic diseases and testing therapeutic interventions. (Blood. 2010;115:1267-1276)

Introduction

Basic mechanisms that underlie platelet production have been elucidated through clinical studies of heritable thrombocytopenia in humans and by investigations of genetically determined platelet disorders in experimental animals. Thrombocytopenia can result from decreased platelet production, production of abnormal platelets, increased destruction, loss as a consequence of hemorrhage, and platelet sequestration.[1] Clinical familial entities that manifest a defect in platelet production or function include more than 100 listings in Online Mendelian Inheritance in Man (OMIM).[2]

Mice bearing spontaneous and genetically engineered mutations have been studied extensively as models for many familial human hematologic and immunologic diseases.[3-5] These mutant mice provide valuable tools to clarify basic physiologic processes and serve as models for experimental interventions that may lead to new treatments. A new spontaneous mutation "thrombocytopenia and cardiomyopathy" *(trac)* occurred in 1987 in the Animal Resources colony of A/J mice at The Jackson Laboratory. Affected animals were small and had shortened life spans. Pathologic and hematologic studies of *trac/trac* mice revealed severe macrothrombocytopenia accompanied by cardiomyopathy and infertility. In this first report of the *trac* mutation we describe the thrombocytopenia and other hematologic defects, determine the chromosomal location of the *trac* locus, identify the molecular basis of the mutation as a model for human hereditary sitosterolemia/phytosterolemia, and document greatly elevated levels of plasma phytosterols. Cardiomyopathy and infertility are the subject of another manuscript (T.H.C. and L.D.S., manuscript in preparation).

Methods

Mice

The *trac* mutation was studied on the A/J strain background and was also backcrossed 10 generations to the BALB/cBy strain. Identification of BALB/cBy +/*trac* heterozygotes during backcrossing was based on polymorphisms at the *D17Mit2* and D17*Mit129* dinucleotide repeat markers that flanked the *trac* locus. C57BL/6J (B6), A/J, BALB/cBy, B6SJL-Tg(*ABCG5/ABCG8*)14-2Hobb/J, and B6;129S6-*Abcg5/Abcg8*^{Tm1Hobb}/J (abbreviated as *(Abcg5/Abcg8)*$^{-/-}$ mice were obtained from the Animal Resources colony at The Jackson Laboratory. After weaning at 3 weeks, all mice were reared on Purina 5K52 diet (6% fat) and acidified water ad libitum. All experimental protocols were approved by The Jackson Laboratory Institutional Animal Care and Use Committee, and are in accordance with accepted institutional and governmental policies.

Ovarian transplants

Ovaries from A/J-*trac/trac* females were transplanted to histocompatible (A/J) or immunodeficient (C3H/JeJ-*Prkdc*^{scid}/*Prkdc*^{scid}) hosts followed by mating to A/J +/+ males. The +/*trac* offspring were then sib-mated. The

Submitted May 5, 2009; accepted September 25, 2009. Prepublished online as *Blood* First Edition paper, October 21, 2009; DOI 10.1182/blood-2009-05-219808.

Presented in part in abstract form at the 47th annual meeting of the American Society of Hematology, Atlanta, Georgia, December 10-13, 2005.[40]

The publication costs of this article were defrayed in part by page charge payment. Therefore, and solely to indicate this fact, this article is hereby marked "advertisement" in accordance with 18 USC section 1734.

mutant and control mice were produced from matings between heterozygotes. Two-thirds of the control mice were expected to be +/*trac* and one-third, +/+. Control mice of the 2 phenotypes are phenotypically indistinguishable and will be referred to as +/? controls.

Transgenic rescue

B6SJL-Tg*(ABCG5/ABCG8)* males were crossed with BALB/cBy +/*trac* females. F1 offspring genotyped as heterozygous for the *trac* mutation and hemizygous for the linked *(ABCG5/ABCG8)* transgenes were crossed with A/J +/*trac* nontransgenic mice. This cross resulted in *trac/trac* Tg*(ABCG5/ABCG8)* mice, *trac/trac* nontransgenic mice, as well as transgenic and nontransgenic +/*trac* and +/+ controls.

Life span determination

Data for life span determination were collected from ages of mice at time of death or age at date of killing for mice that were humanely killed when moribund.

Hematologic measurements

For blood counts and preparation of smears, mice were bled from the retro-orbital sinus with ethylenediaminetetraacetic acid–coated 75-mm capillary tubes (Drummond Scientific). Blood smears were air dried, fixed in methanol, and stained with Wright stain. Complete blood counts,[6] red blood cell (RBC) fragility,[7] and bleeding times[8] were measured as previously described. In cases where bleeding did not stop spontaneously at 5 minutes, it was stopped by application of pressure and bleeding time was recorded as 5 minutes. Platelet activation measured by up-regulation of integrin αIIb β3 (glycoprotein IIb/IIIa, CD41/CD61) was done by flow cytometry using JON/A antibody (Emfret Analytics).[9] Platelet aggregation measurements using bovine collagen as the agonist were performed by impedance-based whole blood in a Chrono-Log Model 700 aggregometer as described.[10] Results were reported as area under the curve.

Histologic examination

After CO_2 asphyxiation, necropsies were carried out and tissues harvested from more than 25 *trac/trac* and +/− control mice at 6 to 17 weeks of age. Tissues were fixed in Bouin solution (LabChem), embedded in paraffin, and sectioned at 5 μm. Tissue sections stained with Mayer hematoxylin and eosin (H&E), or Masson trichrome, were visualized on an Olympus CX41 equipped with a Leica DFC420 digital color camera. Low-power images were scanned with a PathScan Enabler IV (Meyer Instruments; Figure 2A-B), or a Leica DMRXE wide-field microscope (Leica Microsystems) using a PlanApo 100×/1.4 oil objective or a PlanApo 40×/.75 dry objective. Digital images were captured with a Leica DFC300FX camera (Figure 2C-K). Color-subtractive computer-assisted image analysis with ImageJ software (National Institutes of Health [NIH]) of Masson trichrome–stained sections was used as described to quantify percentage of collagen.[11]

To enumerate megakaryocytes in H&E-stained sections of spleen, 3 hot spot areas containing high concentrations of megakaryocytes were identified in the red pulp by visually scanning the entire section of each tissue sample. Megakaryocytes were identified by their large size and characteristic large lobulated basophilic nuclei and abundant cytoplasm.[12] A graticule with 16 squares of 0.25 mm × 0.25 mm was oriented over each hot spot and all megakaryocytes within the grid area were counted at ×200 magnification. The mean number of megakaryocyte counts for each splenic section was calculated by averaging the 3 hot spot counts.

Flow cytometric analyses of megakaryocyte numbers and ploidy

Bone marrow (BM) and spleen cell suspensions were prepared as previously described.[13] Flow cytometric analyses used a Becton Dickinson FACScan equipped with 5-color upgrade by Cytek Development using monoclonal antibodies obtained from BD Pharmingen. Megakaryocytes were identified based on coexpression of CD41 (integrin α2b) and CD61 (integrin β3). Ploidy was determined as previously described.[14]

Immunofluorescence microscopy

Immunofluorescence microscopic analysis of megakaryocytes and analysis of β1-tubulin expression were carried out as described previously.[15] For analysis of platelets, rabbit polyclonal anti–β1-tubulin antibody was a gift of Nick Cowan, New York University. Anti–rabbit secondary antibody was conjugated to Alexa Fluor 488 (Molecular Probes). Platelets were viewed with a Nikon Eclipse TE-2000E microscope using 60× or 100× (NA 1.4) differential interference contrast objectives with a 1.5× optivar. Images were captured with an Orca-II ER cooled CCD camera (Hamamatsu) equipped with an electronic shutter. Shutter and image acquisition were controlled by Metamorph software (Universal Imaging Corporation; Molecular Devices). The diameters of the platelet β1-tubulin coils were measured using the Metamorph software calipers tool.

For analysis of megakaryocytes, rabbit SuperGlu antidetyrosinated tubulin antibody that was a gift from Dr J. Chloe Bulinski (Columbia University, New York, NY) was used at 1:500 dilution. Images were obtained using a Zeiss Axiovert 200 equipped with a 60× differential interference contrast oil-immersion objective.

Transmission electron microscopy

Transmission electron microscopy (TEM) on blood collected from the retro-orbital plexus, bone marrow, and spleen was performed as previously described.[6]

Colony assay for CFU-MK

Numbers of megakaryocyte colony-forming units (CFU-MK) in BM cell suspensions were enumerated using a MegaCult-C kit (StemCell Technologies) formulated for mouse CFU-MKs. Cultures were carried out following the manufacturer's protocol. Cytokine combination used included 50 ng/mL recombinant human thrombopoietin, 10 ng/mL recombinant murine interleukin-3 (IL-3), 20 ng/mL recombinant human IL-6, and 50 ng/mL recombinant human IL-11.

Genetic mapping of the *trac* locus

A/J-*trac/trac* ovary recipient females were mated with C57BL/6 males. The (A/J × C57BL/6) F1 +/*trac* offspring were intercrossed. In the F2 generation, identification of affected homozygous *trac/trac* mice was based on a thin and debilitated appearance and confirmed by histologic evidence of cardiomyopathy and by hematologic evidence of thrombocytopenia. Linkage testing was carried out using dinucleotide repeat polymorphisms (MIT markers) typed by polymerase chain reaction (PCR) amplification. PCR analyses were carried out in 10-μL reactions containing 20 ng of genomic DNA. A DNA pooling strategy facilitated a genome-wide linkage screen. Gene order and recombination frequencies were calculated with the Map Manager computer program, a Macintosh program for storage and analysis of experimental mapping data. For high-resolution mapping, the website http://danio.mgh.harvard.edu/mouseMarkers/musssr.html[16] was used to locate additional simple sequence repeats that differed between the A/J and BL/6 strains. The website was also used to generate DNA sequences of PCR primer pairs for amplification of the new simple sequence repeats.

DNA sequencing and identification of the *trac* mutation

Primers for amplification of candidate gene cDNAs were designed using Primer3 (http://frodo.wi.mit.edu/primer3).[17] Amplified DNA products were treated with ExoSAP-IT (USB Corporation) and sequenced using BigDye Terminators Kit Version 3.1 (Applied Biosystems [ABI]). The subsequent sequencing reactions were cleaned up using ABI's XTerminator solution (ABI) and then run on an ABI 3730xl DNA Analyzer. Sequencing data were analyzed using ABI's Sequencing Analysis software. Sequences were assembled using Sequencher 4.2 (Gene Codes Inc). DNA from mutant mice was analyzed and compared with controls. A 223-bp product containing the G>A mutation was amplified from alkaline lysis–generated genomic DNA. The primers used were forward primer *trac*F, GTCGAGTTCAGCCTGGGTAG and reverse primer *trac*R, GGACACCGCCTTACCAATAA. The

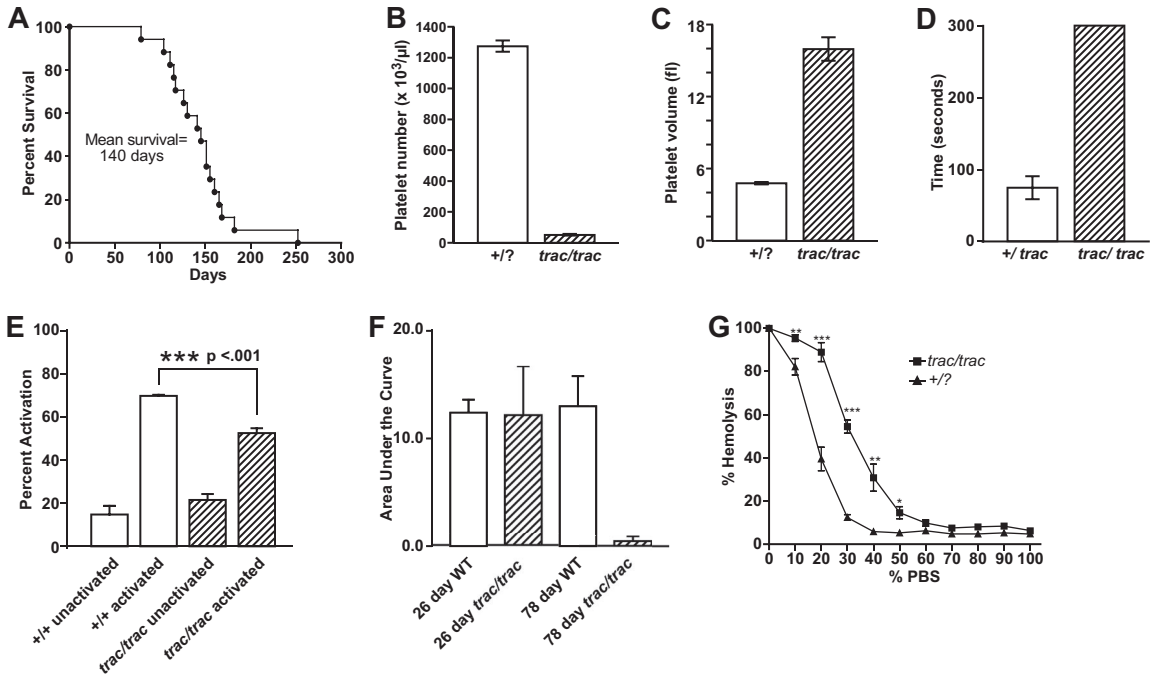

Figure 1. Quantitative abnormalities of A/J-*trac/trac* mice. (A) Survival data showing the short life span of A/J-*trac/trac* mice. There was no significant difference in life span of males and females (n = 18). (B-C) Platelet numbers and platelet volumes in A/J-*trac/trac* and +/? sex-matched littermate mice. Each bar represents the mean and SE from 4 to 9 mice analyzed at 10 to 17 weeks of age. (B) Platelet numbers showing severely reduced counts in A/J-*trac/trac* mice. (C) Platelet volumes showing markedly increased volumes in A/J-*trac/trac* mice. (D) Bleeding times were prolonged in A/J-*trac/trac* mice; n = 5 pairs of 6- to 12-week-old A/J-*trac/trac* and control mice. (E) Platelet activation was impaired in A/J-*trac/trac* mice at 3 to 4 weeks of age (n = 4). (F) In 3-week-old A/J-*trac/trac* mice, platelet aggregation was not significantly different from controls, but by 11 weeks of age they had greatly reduced platelet aggregation performance as measured by the whole blood impedance method. Data show area under the curve using the whole blood impedance method. (G) RBC fragility graph showing increased fragility of A/J-*trac/trac* RBCs (*$P < .05$; **$P < .01$; ***$P < .001$).

product was treated with ExoSAP-IT (USB Corporation) and sequenced to determine the genotype.

Quantitation of plasma sterol levels

Plasma (ethylenediaminetetraacetic acid anticoagulant) was collected for quantification of phytosterol and cholesterol levels. A novel analytic platform based on liquid chromatography/tandem mass spectrometry using atmospheric pressure photoionization enabled the simultaneous quantification of free and esterified β-sitosterol, campesterol, brassicasterol, stigmasterol, and cholesterol.[18] Stock solutions of all phytosterols and cholesterol were prepared in isopropanol.

Development of megakaryocytes from fetal liver cells

Mouse megakaryocytes were cultured as described[19] then resuspended in Dulbecco modified Eagle medium with 10% fetal bovine serum albumin, 50 U/mL penicillin, 50 μg/mL streptomycin, and 0.1 μg/mL purified recombinant human c-Mpl ligand alone, and in the presence of 5% serum from *trac/trac* or +/*trac* mice, and cultured at 37°C before analysis on day 5.

Statistical analyses

Data were expressed as the mean value plus or minus the SE. Significant differences between data groups were determined by 2-sample Student *t* test analysis. A *P* value less than .05 was considered significant.

Results

Occurrence of the trac mutation

The *trac* mutation occurred spontaneously in the A/J inbred strain at The Jackson Laboratory. Affected mice were first identified by their small size and hunched appearance by 12 weeks followed by progressive decline and death by 4 to 6 months of age. Determination of the cause of death as cardiomyopathy, and the presence of thrombocytopenia, led to the naming of the mutation as "thrombocytopenia and cardiomyopathy," with the gene symbol *trac*. Preliminary breeding experiments revealed that both males and females were infertile. Male infertility was associated with defective spermatogenesis. Transfer of ovaries from *trac/trac* females to ovarectomized immunodeficient recipients followed by mating to A/J +/+ males produced +/*trac* mice.

Intercrossing of +/*trac* heterozygotes produced 25% affected mice. Thus *trac* segregated as an autosomal recessive mutation. All homozygous mice developed thrombocytopenia. Thus it is fully penetrant on the A/J strain background. A/J-*trac/trac* homozygotes have a mean life span of 139.8 plus or minus 9.9 days (Figure 1A). There was no effect of sex on life span. A/J +/*trac* breeders survived to at least 8 months, at which time they were killed. There was no effect of heterozygosity at the *trac* locus on platelet numbers or platelet volumes in young (2-3 months) or aged (6-8 months) A/J +/*trac* mice (data not shown).

Effect of the *trac* mutation on peripheral blood counts and bleeding time

Analyses of peripheral blood of A/J-*trac/trac* and sex-matched +/? control mice at 10 to 17 weeks of age showed a 20-fold reduction in platelet numbers ($61.11 \pm 5.7 \times 10^9$/L for *trac/trac* mice vs $1284 \pm 37.1 \times 10^9$/L for littermate controls) accompanied by a 3-fold increased platelet volume (16 ± 1 fL for *trac/trac* mice versus 5 ± .1 fL for littermate controls; Figure 1B-C). There was no significant effect of sex on platelet numbers or volumes in either A/J-*trac/trac* or +/? mice.

The functional effect of the thrombocytopenia was confirmed by greatly increased bleeding times following amputation of the

Table 1. Erythrocyte and leukocyte counts in A/J-*trac/trac* peripheral blood

Genotype	RBC × 10^9/L	RBC MCV, fL	HCT, %	Retics, %	WBC × 10^6/L	Neutrophils, %	Lymphocytes, %
+/?	9.1 ± 0.3	50.0 ± 0.2	45.3 ± 1.4	2.8 ± 0.2	6.7 ± 0.5	13.1 ± 1.3	81.5 ± 1.8
trac/trac	7.5 ± 0.2	48.1 ± 0.8	36.2 ± 0.9	5.9 ± 0.3	2.9 ± 0.3	22.3 ± 2.7	71.1 ± 3.4
P	< .01	< .01	< .03	< .01	< .01	< .05	< .02

Data are based on 9 pairs of A/J-*trac/trac* and sex-matched A/J +/? mice analyzed at 10-17 weeks of age.

tail tip (Figure 1D). Bleeding times for +/? littermate control mice were 78.2 plus or minus 9.9 seconds, compared with bleeding times in excess of 300 seconds for *trac/trac* mice. Functional testing of platelet activation and aggregation revealed decreased platelet activation response in A/J-*trac/trac* mice (Figure 1E), as well as the development of impaired platelet aggregation by 11 weeks of age (Figure 1F).

Young adult A/J-*trac/trac* mice also had mild regenerative hemolytic anemia (hematocrit [Hct] = 36.2% ± 0.9% for *trac/trac* vs 45.3% ± 1.4% for littermate controls), which was accompanied by a doubling in numbers of reticulocytes (5.9% ± 0.3% for *trac/trac* mice vs 2.8% ± 0.2% for littermate controls). Further testing revealed increased RBC fragility in *trac/trac* mice (Figure 1E). A/J-*trac/trac* mice showed a 2-fold reduction in the numbers of white blood cells compared with littermate controls, with an increased percentage of neutrophils and decreased percentages of lymphocytes (Table 1).

Postmortem examination

Postmortem examination showed marked cardiomyopathy with multifocal myocardial fibrosis (Figure 2A-C). Color-subtractive computer-assisted image analysis showed a 7-fold increase in collagen deposition in the myocardium of adult *trac/trac* mice compared with age-matched controls (Figure 2B). There was also spermatic abiotrophy as evidenced by the presence of sperm in testicular tubules and only a few degenerate sperm in the epididymis (not shown). These findings are the subjects of manuscripts in preparation (T.H.C. and L.D.S., manuscript in preparation).

Histologic examination of blood smears

Examination of peripheral blood smears from A/J-*trac/trac* mice at 6 to 10 weeks of age revealed anisocytosis, the presence of stomatocytes, greatly enlarged platelets (Figure 2D-E), and occasional megakaryocytes (Figure 2F). There was no evidence of the inclusions, as has been reported in granulocytes of patients with May-Hegglin anomaly and other giant platelet syndromes[20] either by light or electron microscopy (data not shown).

Further characterization of megakaryocytes and their distribution

Examination of H&E–stained tissue sections showed increased numbers of megakaryocytes in BM (Figure 2G-H), spleen (Figure 2I-J), and lungs (Figure 2K-L) of *trac/trac* mice. Flow cytometric analyses of BM cells from 3 pairs of 4- to 8-week-old *trac/trac* and +/? mice showed a 4-fold increase in percentages of $CD41^+CD61^+$ double-positive megakaryocytes in *trac/trac* (4.3% ± 4.4%) versus +/? (1.1% ± 0.3%) mice ($P < .05$).

Determination of splenic megakaryocyte counts by morphologic criteria in 5 pairs of *trac/trac* and littermate +/? mice at 10 to 15 weeks of age revealed 17.2 plus or minus 6.33 megakaryocytes per field in *trac/trac* mice versus 6.3 plus or minus 0.64 for +/? controls ($P < .001$), a 2.7-fold increase in the number of megakaryocytes in the spleens of *trac/trac* mice. Flow cytometry on spleen cells showed a 5-fold increase in $CD41^+CD61^+$ megakaryocytes in *trac/trac* mice (4.2% ± 4.2% for *trac/trac* mice vs 0.8% ± 0.70% for controls; $P < .05$).

As part of their normal maturation process, megakaryocytes undergo endomitosis 3 to 4 times, resulting in degrees of polyploidy of 16 to 32N. Megakaryocyte ploidy analysis showed that in A/J +/+ control mice there were 3 to 4 endomitoses, resulting in most megakaryocytes being 16N or greater in both BM and spleen, whereas the BM and spleen megakaryocytes of A/J-*trac/trac* mice most commonly underwent only one endomitosis to 4N (Table 2).

β1-Tubulin expression

One of the most prominent features of the resting platelet ultrastructure is a coil of microtubules that defines the periphery of the platelet.[21,22] The increase in size of the *trac/trac* platelets suggested that these microtubule coils may be altered. Examination of β1-tubulin–stained platelets revealed more intense staining and a 1.5-fold increase in the diameter of the microtubule coils of 36-day-old female A/J-*trac/trac* mice, 4.3 plus or minus 0.13 nm versus 2.9 plus or minus 0.09 nm for age- and sex-matched +/? control platelets (Figure 3A-B).

Ultrastructural examination of platelets and megakaryocytes

TEM examination of blood from A/J-*trac/trac* mice revealed greatly enlarged spherical platelets containing increased numbers (per platelet) of small, immature α-granules, increased numbers of mitochondria, and scattered remnants of rough endoplasmic reticulum normally lost during platelet maturation, and lacking normal microtubular elements (Figure 3C-D).

Megakaryocytes from *trac/trac* mice showed absence of a well-defined demarcation membrane system (DMS). Instead of the normal organization of the membranes of the DMS into sheets, there was a change to a spherical or bubblelike appearance. In addition, the endoplasmic reticulum of *trac/trac* megakaryocytes was more prominent and dilated, and there were fewer α-granules, fewer dense bodies, and a wider peripheral zone (not shown; Figure 3E-F).

Platelet numbers and volumes in *trac/trac* mice are normal at weaning

Hematologic analyses at weaning (18-21 days of age) of litters born from A/J +/*trac* breeders revealed normal platelet counts and volumes. However, within a few weeks after weaning, hematologic analyses of A/J-*trac/trac* mice showed a precipitous drop in platelet counts (Figure 4A) and marked increase in platelet volumes (Figure 4B).

Numbers of megakaryocyte progenitors are increased 2-fold in *trac/trac* bone marrow

To quantify numbers of megakaryocyte progenitors, colony assays were carried out in BM from 5 pairs of A/J-*trac/trac* and +/? mice

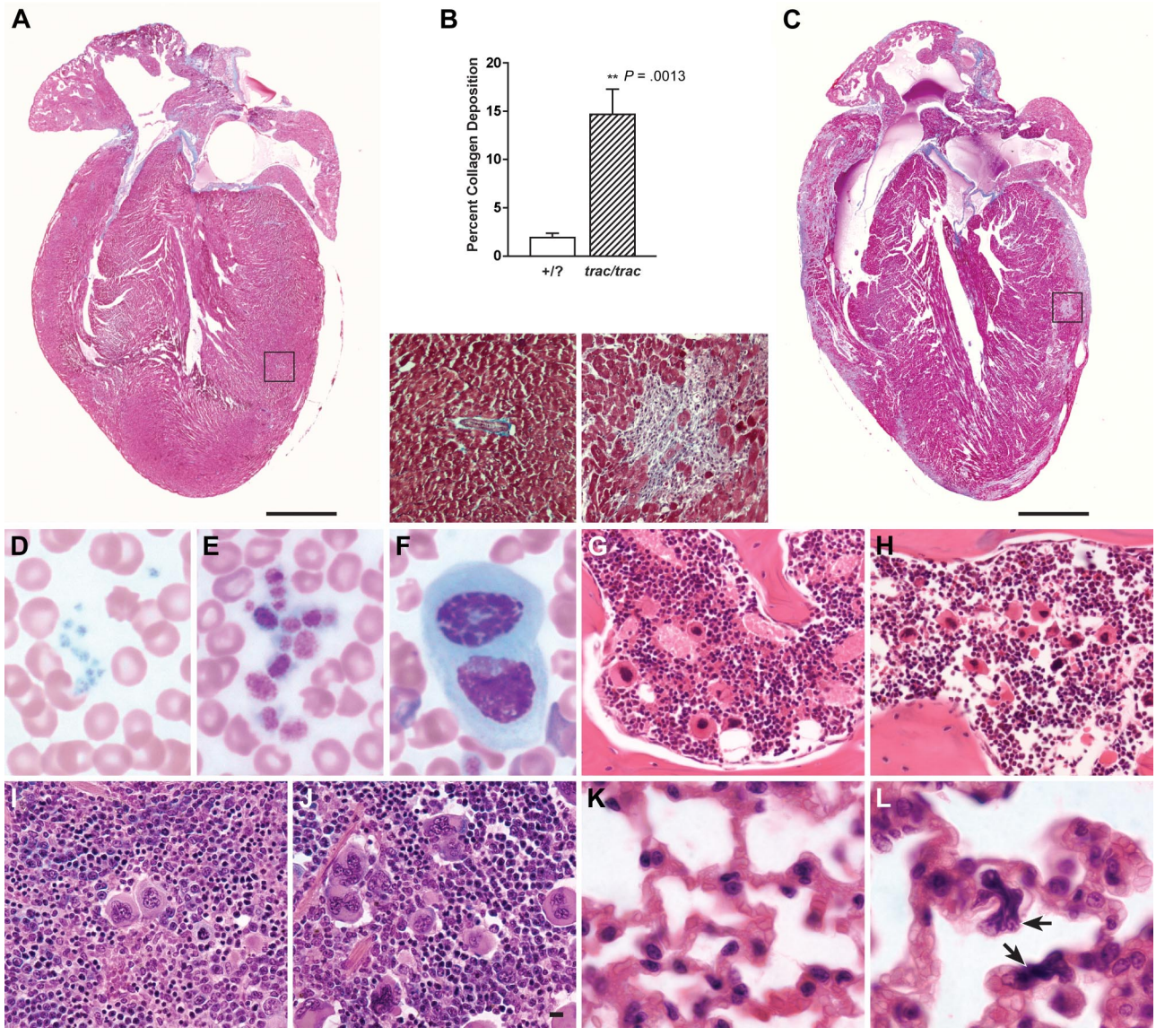

Figure 2. Histopathologic and hematologic abnormalities of A/J-*trac/trac* mice. (A) Heart and myocardium (inset) of A/J +/? control mouse showing normal structure, higher magnification insets of boxed areas. (B) Determination of collagen deposition in heart ventricles by color-subtractive computer-assisted image analysis showed a mean of 1.9% collagen in A/J +/? controls and 14.6% in A/J-*trac/trac* mice, a 7-fold increase in collagen deposition (n = 5). (C) Heart and myocardium (inset) of A/J-*trac/trac* mouse showing cardiomyopathy with severe multifocal fibrosis. (D-L) Peripheral blood smears and histopathology of BM, spleen, and lungs. (D-F) Blood smears of A/J-*trac/trac* and +/? control mice at 10 weeks of age. (D) A/J +/? mouse blood smear showing normal platelet size. (E) A/J-*trac/trac* blood smear showing greatly enlarged platelets. (F) A/J-*trac/trac* blood smear showing megakaryocyte. (G-H) Vertebral BM at 15 weeks. (G) A/J +/? BM showing normal distribution of megakaryocytes. (H) A/J-*trac/trac* BM showing increased numbers of megakaryocytes. (I-J) Red pulp of spleen. (I) A/J +/? spleen showing normal distribution of megakaryocytes. (J) A/J-*trac/trac* spleen showing increased numbers of megakaryocytes. (K-L) Lungs. (K) A/J +/? lungs showing normal structure. (L) A/J-*trac/trac* lungs showing megakaryocytes in alveolar capillary bed (arrows). (A,C) Masson trichrome stain; bars represent 1 mm. (D-F) Wright stain. (G-L) Hematoxylin and eosin; bars represent 10 μm.

Table 2. Comparison of A/J-*trac/trac* polyploidy with that of littermate controls A/J +/+

Genotype/tissue	4N	8N	16N	More than 16N
+/+ BM	10 ± 2	9 ± 4	22 ± 8	12 ± 4
+/+ spleen	16 ± 2	5 ± 1	13 ± 1	40.2 ± 6
trac/trac BM	15 ± 1*	4 ± 0	8 ± 2*	8 ± 3
trac/trac spleen	63 ± 3†	7 ± 1	1 ± 0†	5 ± 0†

Values are percentage of $CD41^+$ cells.
BM indicates bone marrow.
*Significantly different than +/+ BM ($P < .05$).
†Significantly different than +/+ spleen ($P < .001$).

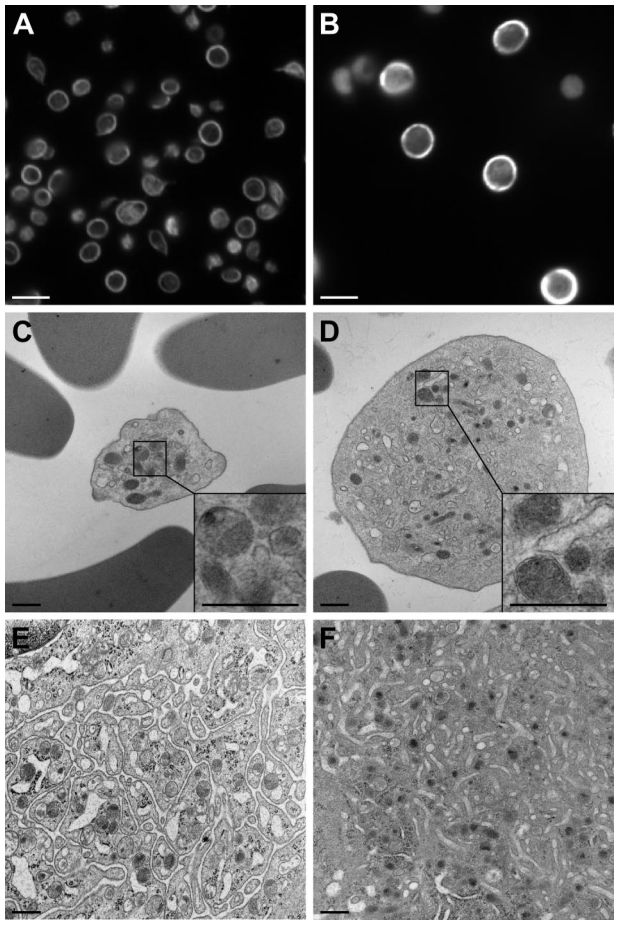

Figure 3. Immunofluorescent and transmission electron microscopic changes in platelets and megakaryocytes. (A-B) Immunofluorescence photomicrographs of platelets stained with anti–β1-tubulin antibody at 1000 ×; bars represent 5 μM. (A) A/J +/? control platelets showing normal β1-tubulin immunoreactivity. (B) Enlarged A/J-*trac/trac* platelets showing increased β1-tubulin immunoreactivity. (C-F) TEM of platelets and megakaryocytes. (C) A/J +/+ platelet showing normal structure. (D) A/J-*trac/trac* platelet showing large size, numerous small alpha granules, and increased numbers of mitochondria in each platelet. (E) A/J +/+ megakaryocyte showing well-developed platelet demarcation membrane system (DMS). (F) A/J-*trac/trac* megakaryocyte showing altered DMS. (C-F) Bars represent 500 nM.

at 19 to 34 weeks of age. Numbers of colonies per culture dish were 23.4 plus or minus 1.50 for A/J-*trac/trac* mice versus 12.2 plus or minus 1.30 for +/− controls ($P = .002$).

High-resolution mapping of the *trac* locus

Genetic crosses were carried out to determine the chromosomal location of the *trac* mutation. Recipients of A/J-*trac/trac* ovaries were first mated with C57BL/6J (B6) +/+ males. Intercrossing of male and female (A/J × B6) F1 +/*trac* heterozygotes produced 1102 F2 progeny. Identification of 277 *trac/trac* homozygotes (25.14%) was based on the presence of thrombocytopenia. The flanking MIT markers *D17Mit155* at 84.4 Mb and *D17Mit76* at 85.5 Mb narrowed the interval to 1.1 Mb, which included 17 genes. Custom primer sets were then designed to genotype 3 additional simple sequence repeat markers that narrowed the interval to 0.3 Mb, which contained only 4 genes: dynein 2 light intermediate chain *(D2lic)*; adenosine triphosphate (ATP)–binding cassette, subfamily G (WHITE), member 5 *(Abcg5)*; ATP-binding cassette, subfamily G (WHITE), member 8 *(Abcg8)*; and leucine-rich PPR-motif containing *(Lrpprc)*.

Sequencing of candidate genes and identification of *Abcg5* as the disrupted gene

Sequencing of the cDNA from the 4 genes within the interval revealed a G to A mutation at base 1435 of *Abcg5* (reference sequence NM_031884.1; Figure 5A-B). No DNA alterations were found in any of the other candidate genes within the interval. The G to A base substitution changes a tryptophan to a premature stop codon (UGG to UAG). The transmembrane helices prediction program TMHMM Version 2.0 (http://www.cbs.dtu.dk/services/TMHMM)[24] predicts that the premature stop codon would result in a mutant protein that lacks the last 4 transmembrane domains of the wild-type protein (Figure 5C black box).

Transgenic rescue of thrombocytopenia

To determine whether expression of a normal *ABCG5* transgene could rescue thrombocytopenia in *trac/trac* mice, crosses between mice doubly transgenic for the tightly linked human *ABCG5* and *ABCG8* genes and +/*trac* heterozygotes were carried out. These crosses produced mice that were transgenic for the *ABCG5* and *ABCG8* genes (referred to as *(ABCG5/ABCG8)* and homozygous for the *trac* mutation along with nontransgenic *trac/trac* mice and transgenic control (+/*trac* or +/+ *ABCG5/ABCG8*) animals. The transgenic mice are maintained on a segregating B6SJL strain background and have approximately 10 copies of the human *ABCG5* and *ABCG8* genes under the direction of their endogenous regulatory sequences.[25] For genetic crosses with the transgenic mice, we used a stock of BALB/cBy-*trac* mice created by crossing the *trac* mutation for 10 generations from the A/J strain onto the BALB/cBy strain background. As shown in Table 3 and Figure 6, homozygous mutant (BALB/cBy × B6SJL)-*trac/trac* mice that also inherited the *ABCG5* and *ABCG8* transgenes have normal platelet counts and platelet volumes, whereas the nontransgenic (BALB/cBy × B6SJL)-*trac/trac* mice, as expected, showed severe macrothrombocytopenia.

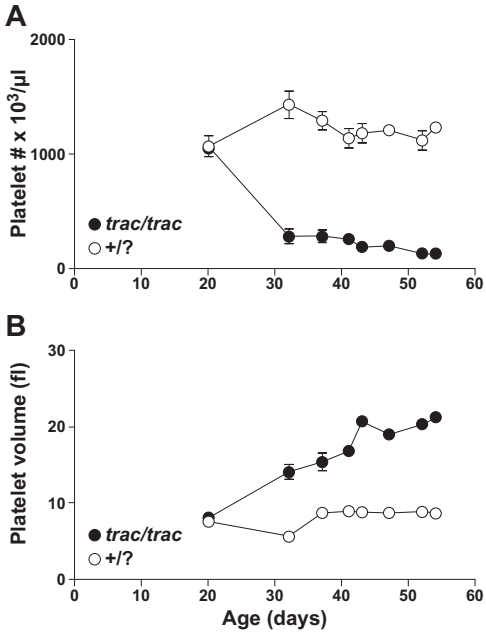

Figure 4. Change in platelet numbers and volumes of A/J-*trac/trac* mice after weaning. (A) Platelet numbers showing a marked decline in A/J-*trac/trac* platelet numbers at 3 to 5 weeks of age. (B) Platelet volumes showing a marked increase in A/J-*trac/trac* platelet volumes at 3 to 5 weeks of age.

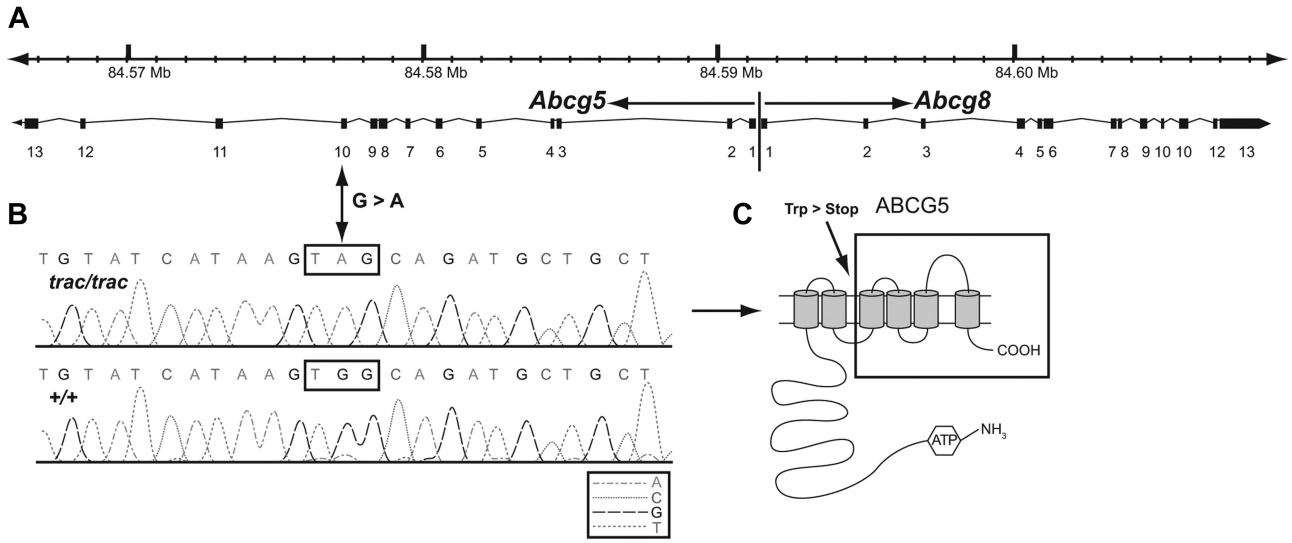

Figure 5. Genomic structure of the *Abcg5* and *Abcg8* genes showing the site and nature of the *trac* mutation. (A) *Abcg5* and *Abcg8* are arranged tandemly head to head in opposite transcriptional orientations (arrows) and span ~ 42 kb on mouse chromosome 17 from position 84.567 Mb to 84.609 Mb (National Center for Biotechnology Information build 36)[23] as shown in the scale at the top of the figure. Individual exons of each gene are numbered and represented as filled rectangles and introns are represented as connecting lines. (B) The *trac* mutation is a G to A base pair substitution in exon 10 of the *Abcg5* gene. The mutation changes a UGG tryptophan (Trp) codon in wild-type (+/+) mice to a UGA stop codon in mutant (*trac/trac*) mice. (C) The normal mouse ABCG5 protein (NP_114090) is composed of 652 amino acids and contains 6 predicted transmembrane domains (gray cylinders). The premature stop codon introduced by the *trac* mutation at amino acid position 462 is predicted to truncate the protein after the second transmembrane domain and eliminate 190 amino acids containing 4 additional transmembrane domains (region enclosed in black box).

Mice homozygous for the *Abcg5/Abcg8* targeted mutations develop macrothrombocytopenia

Previous reports on *Abcg5/Abcg8* double knockout mice maintained on a segregating strain background did not include examination of platelet levels.[26-28] Examination of platelet counts and volumes from 4 pairs of B6;129-$(Abcg5/Abcg8)^{-/-}$ and littermate control $(Abcg5/Abcg8)^{+/?}$ heterozygous mice at 5 to 7 months of age showed marked macrothrombocytopenia in the $(Abcg5/Abcg8)^{+/?}$ mice (Table 4). There was no significant difference between the $(Abcg5/Abcg8)^{-/-}$ and littermate control $(Abcg5/Abcg8)^{+/?}$ heterozygotes in either RBC or leukocyte counts (data not shown).

Effect of the *trac* mutation on plasma phytosterol levels

ABCG5 and ABCG8 are obligate hemitransporters and form a functional complex that limits the accumulation of dietary phytosterols,[29,30] which are common components of plant foods especially vegetable oils, seeds, nuts, and cereals.[18] They are structurally similar to cholesterol, differing only in the number of carbons and/or double bonds in the side chains.[18] Mutations in either the *ABCG5* or *ABCG8* genes result in phytosterolemia, a rare inherited condition characterized by increased levels of plasma and tissue plant sterols due to higher intestinal absorption and impaired biliary secretion of phytosterols.[31]

Disruption of the *Abcg5* gene by the *trac* mutation predicts elevated levels of sitosterol and other phytosterols in the plasma of *trac/trac* mice. As shown in Table 5, A/J-*trac/trac* plasma showed an approximately 130-fold and approximately 60-fold increase in free and esterified sitosterol, respectively, compared with A/J +/? control mice. Plasma levels of other plant sterols including free and esterified stigmasterol, brassicasterol, and campesterol were also significantly elevated. There was no effect of the *trac* mutation on levels of free cholesterol. However, levels of esterified cholesterol were decreased to approximately one-half those found in plasma from littermate normal +/? controls.

A/J-*trac/trac* phytosterol-rich serum interferes with development of megakaryocytes in normal fetal liver cell cultures

Megakaryocytes generate platelets by remodeling their cytoplasm into long proplatelet extensions, which serve as assembly lines for platelet production.[15] To test the hypothesis that the presence of heightened phytosterol levels interferes with normal development of megakaryocytes and production of proplatelets, normal fetal mouse liver megakaryocytes were cultured in the presence of A/J-*trac/trac* or +/? serum. The finding that the microenvironmental defect resulting in thrombocytopenia was associated with greatly elevated serum phytosterol levels suggests that addition of *trac/trac* serum into normal fetal liver megakaryocyte cultures would result in abnormal proplatelet production. When fetal liver megakaryocytes from embryonic day 13 CD1 mouse fetuses were cultured in the presence of serum (5%) obtained from adult phytosterolemic A/J-*trac/trac* mice, there was a 63% reduction in the number of proplatelet-producing megakaryocytes: 26% plus or minus 4.2% in the presences of A/J-*trac/trac* serum versus 71% plus or minus 7.2% in A/J +/? control serum (Figure 7).

Table 3. Human *ABCG5/ABCG8* transgenic rescue of the *trac* mutation

Genotype	*+/? +/+* N = 4	*+/? +/TgN** N = 3	*trac/trac +/+* N = 3	*trac/trac +/TgN** N = 5
Platelet no., $\times 10^9$/L	1048 ± 110	1165 ± 125	248 ± 58	1102 ± 79†
Platelet volume, fL	7.1 ± 0.7	7.5 ± 1.2	20.5 ± 2.4	6.9 ± 1.0†

*TgN is an abbreviation of genotype for the *ABCG5*- and *ABCG8*-linked human transgenes.

†Platelet counts and volumes significantly different from those of *trac/trac* +/+ (nontransgenic) mice at $P < .001$.

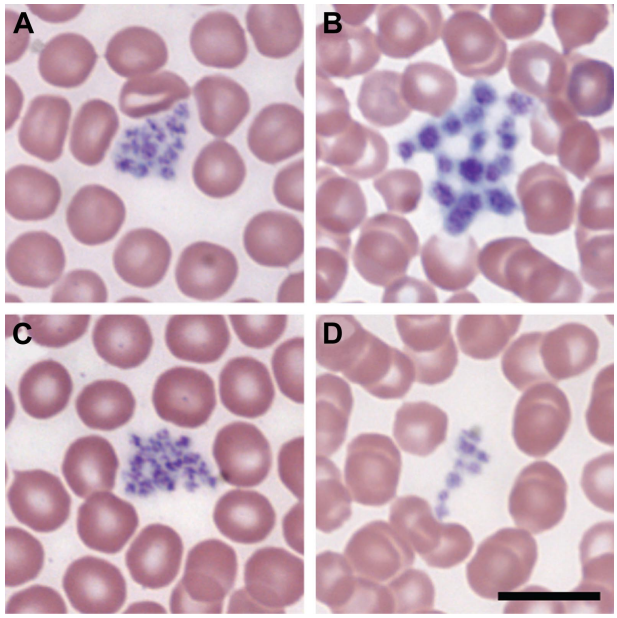

Figure 6. Blood smears showing transgenic rescue of thrombocytopenia. (A) A/J +/+ +/+ with normal-sized platelets, (B) A/J-*trac/trac* +/+ with enlarged platelets, (C) A/J +/+ Tg *(ABCG5/8)* with normal-sized platelets, and (D) A/J-*trac/trac* Tg *(ABCG5/8)* with normal-sized platelets. Bar represents 10 μm.

Discussion

In this paper we describe the *trac* mutation characterized clinically as causing thrombocytopenia and cardiomyopathy. This is the first description of a spontaneous single-gene mouse mutation at the *Abcg5* gene resulting in a wide range of pathophysiologic effects that present a clinically significant model for human hereditary phytosterolemia. The most striking hematologic effect of the *trac* mutation is a 20-fold reduction in platelet numbers accompanied by a 3-fold increased platelet size that occurs rapidly after weaning. TEM revealed that these large platelets lack normal microtubular coils and contain increased numbers of small, immature α-granules, increased numbers of mitochondria in each platelet, and scattered remnants of organelles such as rough endoplasmic reticulum that are normally lost during platelet maturation. Immunofluorescence microscopy showed that the β1-tubulin coils had a 2-fold increase in diameter. Prolonged bleeding times confirmed that there was also a functional defect in hemostasis. Platelet functional testing revealed that these large abnormal platelets have an impaired activation response as determined by flow cytometric assays and by 11 weeks of age lose the ability to aggregate normally as tested in whole blood by the impedance method.

In adult mice platelets are produced by megakaryocytes in the BM and spleen. Flow cytometry and cytologic enumeration showed that the thrombocytopenia in A/J-*trac/trac* mice was paradoxically associated with increased numbers of splenic and BM megakaryocytes. Normal megakaryocytes undergo endocytosis 3 to 4 times, resulting in polyploidy of 16N to 32N. However, in *trac/trac* mice megakaryocytes typically undergo only one round of endomitosis, resulting in reduced polyploidy. Megakaryocytes normally generate platelets by remodeling their cytoplasm into long, branched proplatelets, which serve as assembly lines for platelet production. The formation of elongated proplatelet intermediates is normally accompanied by a large increase in total surface area. One of the hallmark features of mature megakaryocytes is a highly invaginated membrane system, called the demarcation membrane system (DMS). The DMS functions to provide a membrane reserve that undergoes evagination during the formation of proplatelets. Thus, the reorganization of this membrane system is crucial for proplatelet extension and platelet production.[32,33] Ultrastructurally, these intricate membranes have the appearance of very long narrow parallel membranes. In *trac/trac* megakaryocytes, there is a poorly developed DMS that appears ultrastructurally as short sections of dilated DMS, often spherical in appearance. In normal megakaryocytes membranous strands wrap β1-tubulin coils and cytoplasmic material to form discoid platelets 2 to 3 micrometers in diameter, containing the granules and other subcellular components of the normal platelet. The defect in *trac/trac* megakaryocytes results in the production of exceedingly large, spherical platelets, in severely reduced numbers, and in prolonged bleeding times.

In addition to the platelet and megakaryocyte abnormalities, A/J-*trac/trac* mice had increased RBC fragility resulting in a mild hemolytic anemia with a regenerative response, evidenced by a doubling of the reticulocyte count. This RBC fragility is consistent with a reduction in the durability of the RBC membrane. There was also a 50% reduction in the leukocyte count due mostly to decreased numbers of lymphocytes. We identified other, nonhematogenous abnormalities including cardiomyopathy and infertility that will be the subjects of separate manuscripts (T.H.C. and L.D.S., manuscript in preparation).

Initial breeding experiments showed that both A/J-*trac/trac* males and females were infertile. The female infertility is not due to a germ cell defect since engraftment of ovaries from *trac/trac* females to immunodeficient recipients followed by mating to A/J +/+ males produced A/J +/*trac* mice. Results of intercrossing +/*trac* heterozygotes indicated that the *trac* mutation segregated as an autosomal recessive mutation. High-resolution mapping of the *trac* locus and sequencing of candidate genes revealed a G to A transition in the *Abcg5* gene, and no DNA alterations in any of the other 3 genes within the candidate interval. This G to A substitution results in a premature stop codon and predicts a truncated protein that lacks the last 4 transmembrane domains of the wild-type protein, resulting in a defective ABCG5/ABCG8 heterodimer.

The ABCG5/ABCG8 heterodimer mediates the efflux of plant sterols and cholesterol from enterocytes into the intestinal lumen and the secretion of phytosterols from hepatocytes into the bile,[31,34] thus limiting the accumulation of dietary phytosterols,[29,30] which are common components of plant foods especially vegetable oils, seeds, nuts, and cereals.[18] Mutations in either the human *ABCG5* or *ABCG8* genes are known to result in phytosterolemia.[35]

Phytosterols are structurally similar to cholesterol, differing only in the number of carbons or double bonds in the side chains.[18] Cholesterol is one of the major lipid constituents of red blood cell membranes and functions in membrane permeability, fluidity, and rigidity.[36,37] Significant alterations in the fluidity or durability of membranes may occur when phytosterols are incorporated.

Homozygosity for this spontaneous mutation in the *Abcg5* gene results in pathologically high levels of plant sterol absorption on

Table 4. Macrothrombocytopenia in mice doubly homozygous for the *Abcg5/Abcg8*-targeted mutations

Genotype	Platelet number, × 10^9/L	MPV, fL
(*Abcg5/Abcg8*)$^{-/-}$	335 ± 103*	14.8 ± 2.1*
(*Abcg5/Abcg8*)$^{+/?}$	1201 ± 159	5.1 ± 0.4

Data are from 4 pairs of targeted mutant (−/−) and heterozygous littermate control mice examined at 5-7 months of age.

*(*Abcg5/Abcg8*)$^{-/-}$ mice significantly different from (*Abcg5/Abcg8*)$^{+/?}$ controls at $P < .01$.

Table 5. Plasma sterol levels in A/J-*trac/trac* mice

	Sitosterol		Brassicasterol		Campesterol		Stigmasterol		Cholesterol	
Genotype	Free	Esterified	Free	Esterified	Free	Esterified	Free	Esterified	Free	Esterified
trac/trac, N = 9	250.7 ± 17	624.4 ± 50	10.8 ± 1.3	11.6 ± 2.0	96.3 ± 7.3	237.4 ± 21.9	36.1 ± 1.5	49.2 ± 4.0	143.1 ± 9.9	493.3 ± 48
+/?, N = 14	1.9 ± 0.3	10.6 ± 1.4	0.8 ± 0.1	2.5 ± 0.2	5.6 ± 0.9	29.0 ± 4.0	0.3 ± 0.0	0.8 ± 0.1	135.3 ± 10.9	904.3 ± 61.8
Fold change	131	59	13.5	4.6	17	8	120	62	1.05	−1.8
P	< .001	< .001	< .001	< .001	< .001	< .001	< .001	< .001	ns	< .001

Values presented as milligrams per liter (mg/L) in A/J-*trac/trac* and +/? littermate control mice tested at 8-17 weeks of age.

commonly used plant sterol–containing rodent diets. The measurement of blood levels of phytosterols in *trac/trac* mice showed an approximately 130-fold increase in free and approximately 60-fold increase in esterified sitosterol as well as significant elevations of free and esterified brassicasterol, campesterol, and sigmasterol. Although hypercholesterolemia is a feature of sitosterolemia in humans, there was no effect of the *trac* mutation on levels of free cholesterol, and levels of esterified cholesterol were decreased to approximately one half those found in plasma from littermate normal +/? controls. To confirm the link between phytosterolemia and abnormal thrombopoiesis, normal fetal megakaryocytes were cultured in normal and phytosterol-rich environments. Results showed a 63% reduction in the number of proplatelet-producing megakaryocytes when cultured in the presence of 5% A/J-*trac/trac* serum compared with culture in 5% A/J +/*trac* serum.

To corroborate the causative nature of the *Abcg5* gene in *trac/trac* mice, we showed that the thrombocytopenia could be rescued by the human *ABCG5/ABCG8* transgenes. We also showed that mice homozygous for the *Abcg5/Abcg8* targeted mutation developed macrothrombocytopenia secondary to phytosterolemia. Recently, Kruit et al[38] reported that mice homozygous for an *Abcg5* targeted mutation develop macrothrombocytopenia accompanied by sitosterolemia. Treatment with ezetimibe to inhibit sterol absorption decreased sitosterol levels and reversed the macrothrombocytopenia. Our laboratory has found that providing *trac/trac* mice with a phytosterol-free diet also normalized platelet levels, and rescued other pathologic changes associated with phytosterolemia in these mice (T.H.C. and L.D.S., manuscript in preparation).

There were several differences between the findings in the *Abcg5* targeted mutation studied by Kruit et al, and our findings in the spontaneous *trac* mutation. They reported an absence of RBC fragility in the *Abcg5* knockout mice. We found that in the phytosterolemia of A/J-*trac/trac* mice, as in human phytosterolemia,[35,39] there is red blood cell fragility and low-level hemolysis. Kruit et al also reported no change in megakaryocyte ploidy, whereas we found that there was a decrease in the polyploidy in *trac/trac* mice. In the *Abcg5* targeted mutant mouse they did not find abnormalities in leukocyte populations, whereas we found a significant decrease in lymphocyte numbers in *trac/trac* mice. The cardiomyopathy and the spermatic abiotrophy that are prominent features in this spontaneous *trac* mutation were not reported in their targeted mutation. These differences could be due in part to strain background effects.

Although much is known about the role of ABCG5 as a heterodimeric partner in the uptake of plant sterols and cholesterol, the understanding of mechanisms by which these plant sterols interfere with development of membranes that depend on cholesterol and cholesterol metabolism is incomplete. It seems likely that mechanisms to exclude plant sterols from mammalian metabolism evolved because, although structurally very similar to cholesterol, there appear to be inherent disadvantages in the incorporation of these stoichemically different molecules into various membranes. The spontaneous *trac* mutation provides a model to extend investigations of mechanisms by which plant sterols interfere with megakaryocytopoiesis and the formation of platelets, red blood cells, cardiomyocytes, and other affected cells. Ongoing studies

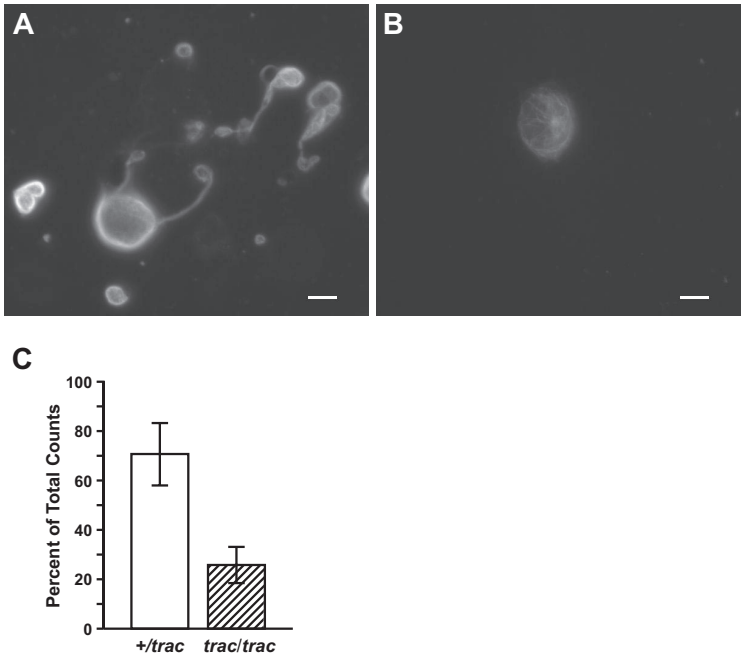

Figure 7. Generation of proplatelets from normal mouse fetal liver cultures. (A) Appearance of normal fetal liver megakaryocytes generating normal proplatelet processes when cultured with 5% A/J +/+ sera. (B) Appearance of normal fetal liver megakaryocytes cultured with 5% A/J-*trac/trac* sera failing to generate proplatelet processes. Representative samples were stained with rabbit polyclonal antibody SUP GLU, diluted 1:1000, which recognizes detyrosinated tubulin. Bar represents 5 μm. (C) Seventy-one percent of normal fetal liver megakaryocytes generated proplatelet processes when cultured with 5% A/J +/+ sera versus 26% when cultured with 5% A/J-*trac/trac* sera.

will identify targets for therapeutic intervention in the treatment of macrothrombocytopenia due to phytosterolemia.

Acknowledgments

We gratefully acknowledge Nick Cowan (New York University) for providing anti–β1-tubulin antibody, and Chlöe Bulinski for the kind gift of pAb SUP GLU. We thank David Serreze and Luanne Peters for critical review of the manuscript.

This work was supported by National Institutes of Health (NIH) grants (T32) RR-070 68-07TC (T.H.C.); HL-077642 (L.D.S.); and HL-68130 (J.E.I.); and NIH Cancer Core Grant CA-34196 to The Jackson Laboratory.

Authorship

Contribution: P.L. discovered the mutant mouse; P.L. and B.H. investigated the inheritance; T.H.C., B.L.L., L.R.D., L.M.B., B.G., U.C., J.T., H.W., J.N.T., and L.D.S. performed the experiments; R.T.B. and O.F. carried out the histopathologic studies; T.H.C., B.L.L., L.M.B., J.N.T., J.E.I., K.R.J., and L.D.S. analyzed data and results; T.H.C., J.E.I., K.R.J., and L.D.S. designed the research; and T.H.C. and L.D.S. wrote the paper.

Conflict-of-interest disclosure: The authors declare no competing financial interests.

Correspondence: Leonard D. Shultz, The Jackson Laboratory, 600 Main St, Bar Harbor, ME; e-mail: lenny.shultz@jax.org.

References

1. Angiolillo A, Luban N. *Platelet Transfusion in Infants and Children*. In: Michelson AD, ed. Platelets. Academic Press: San Diego, CA; 2002:907-914.
2. McKusick VA. Mendelian Inheritance in Man and its online version, OMIM: McKusick-Nathans Institute of Genetic Medicine, Johns Hopkins University (Baltimore, MD), and National Biotechnology Information. http://www.ncbi.nlm.nih.gov/omim. Accessed July 2008.
3. Russell ES. Developmental studies of mouse hereditary anemias. *Am J Med Genet.* 1984;18(4):621-641.
4. Shultz LD, Sidman CL. Genetically determined murine models of immunodeficiency. *Annu Rev Immunol.* 1987;5367-5403.
5. Joliat MJ, Shultz LD. The molecular bases of spontaneous immunological mutations in the mouse and their homologous human diseases. *Clin Immunol.* 2001;101(2):113-129.
6. Robledo RF, Ciciotte SL, Gwynn B, et al. Targeted deletion of alpha-adducin results in absent beta- and gamma-adducin, compensated hemolytic anemia, and lethal hydrocephalus in mice. *Blood.* 2008;112(10):4298-4307.
7. Lyons BL, Lynes MA, Burzenski L, Joliat MJ, Hadjout N, Shultz LD. Mechanisms of anemia in SHP-1 protein tyrosine phosphatase-deficient "viable motheaten" mice. *Exp Hematol.* 2003;31(3):234-243.
8. Chrzanowska-Wodnicka M, Smyth SS, Schoenwaelder SM, Fischer TH, White GC II. Rap1b is required for normal platelet function and hemostasis in mice. *J Clin Invest.* 2005;115(3):680-687.
9. Emfret Analytics. http://www.emfret.com/protocols.htm. Accessed August 15, 2009.
10. Dyszkiewicz-Korpanty AM, Frenkel EP, Sarode R. Approach to the assessment of platelet function: comparison between optical-based platelet-rich plasma and impedance-based whole blood platelet aggregation methods. *Clin Appl Thromb Hemost.* 2005;11(1):25-35.
11. Gaspard GJ, Pasumarthi KB. Quantification of cardiac fibrosis by colour-subtractive computer-assisted image analysis. *Clin Exp Pharmacol Physiol.* 2008;35(5-6):679-686.
12. Chenaille PJ, Steward SA, Ashmun RA, Jackson CW. Prolonged thrombocytosis in mice after 5-fluorouracil results from failure to down-regulate megakaryocyte concentration: an experimental model that dissociates regulation of megakaryocyte size and DNA content from megakaryocyte concentration. *Blood.* 1990;76(3):508-515.
13. Shultz LD, Lang PA, Christianson SW, et al. NOD/LtSz-Rag1null mice: an immunodeficient and radioresistant model for engraftment of human hematolymphoid cells, HIV infection, and adoptive transfer of NOD mouse diabetogenic T cells. *J Immunol.* 2000;164(5):2496-2507.
14. Jackson CW, Brown LK, Somerville BC, Lyles SA, Look AT. Two-color flow cytometric measurement of DNA distributions of rat megakaryocytes in unfixed, unfractionated marrow cell suspensions. *Blood.* 1984;63(4):768-778.
15. Italiano JE Jr, Lecine P, Shivdasani RA, Hartwig JH. Blood platelets are assembled principally at the ends of proplatelet processes produced by differentiated megakaryocytes. *J Cell Biol.* 1999;147(6):1299-1312.
16. Massachusetts General Hospital. Mouse genome build m37. http://danio.mgh.harvard.edu/mouseMarkers/musssr.html. Accessed June 2006.
17. Howard Hughes Medical Institute, National Institutes of Health, National Human Genome Research Institute. Primer3. http://frodo.wi.mit.edu/primer3. Accessed June 2006.
18. Lembcke J, Ceglarek U, Fiedler GM, Baumann S, Leichtle A, Thiery J. Rapid quantification of free and esterified phytosterols in human serum using APPI-LC-MS/MS. *J Lipid Res.* 2005;46(1):21-26.
19. Flaumenhaft R, Dilks JR, Richardson J, et al. Megakaryocyte-derived microparticles: direct visualization and distinction from platelet-derived microparticles. *Blood.* 2009;113(5):1112-1121.
20. Mhawech P, Saleem A. Inherited giant platelet disorders: classification and literature review. *Am J Clin Pathol.* 2000;113(2):176-190.
21. White JG. Effects of colchicine and vinca alkaloids on human platelets, II: changes in the dense tubular system and formation of an unusual inclusion in incubated cells. *Am J Pathol.* 1968;53(3):447-461.
22. Patel-Hett S, Richardson JL, Schulze H, et al. Visualization of microtubule growth in living platelets reveals a dynamic marginal band with multiple microtubules. *Blood.* 2008;111(9):4605-4616.
23. National Center for Biotechnology Information. Build 36. http://www.ncbi.nlm.nih.gov/mapview/map_search.cgi?taxid=10090. Accessed .
24. Center for Biological Sequence Analysis. TMHMM Server V 2.0. http://www.cbs.dtu.dk/services/TMHMM. Accessed .
25. Yu L, Li-Hawkins J, Hammer RE, et al. Overexpression of ABCG5 and ABCG8 promotes biliary cholesterol secretion and reduces fractional absorption of dietary cholesterol. *J Clin Invest.* 2002;110(5):671-680.
26. Graf GA, Yu L, Li WP, et al. ABCG5 and ABCG8 are obligate heterodimers for protein trafficking and biliary cholesterol excretion. *J Biol Chem.* 2003;278(48):48275-48282.
27. Yu L, Hammer RE, Li-Hawkins J, et al. Disruption of Abcg5 and Abcg8 in mice reveals their crucial role in biliary cholesterol secretion. *Proc Natl Acad Sci U S A.* 2002;99(25):16237-16242.
28. Yu L, von Bergmann K, Lutjohann D, Hobbs HH, Cohen JC. Ezetimibe normalizes metabolic defects in mice lacking ABCG5 and ABCG8. *J Lipid Res.* 2005;46(8):1739-1744.
29. Berge KE, Tian H, Graf GA, et al. Accumulation of dietary cholesterol in sitosterolemia caused by mutations in adjacent ABC transporters. *Science.* 2000;290(5497):1771-1775.
30. Graf GA, Cohen JC, Hobbs HH. Missense mutations in ABCG5 and ABCG8 disrupt heterodimerization and trafficking. *J Biol Chem.* 2004;279(23):24881-24888.
31. Lu K, Lee MH, Hazard S, et al. Two genes that map to the STSL locus cause sitosterolemia: genomic structure and spectrum of mutations involving sterolin-1 and sterolin-2, encoded by ABCG5 and ABCG8, respectively. *Am J Hum Genet.* 2001;69(2):278-290.
32. Radley JM, Haller CJ. The demarcation membrane system of the megakaryocyte: a misnomer? *Blood.* 1982;60(1):213-219.
33. Schulze H, Korpal M, Hurov J, et al. Characterization of the megakaryocyte demarcation membrane system and its role in thrombopoiesis. *Blood.* 2006;107(10):3868-3875.
34. Hubacek JA, Berge KE, Cohen JC, Hobbs HH. Mutations in ATP-cassette binding proteins G5 (ABCG5) and G8 (ABCG8) causing sitosterolemia. *Hum Mutat.* 2001;18(4):359-360.
35. Su Y, Wang Z, Yang H, et al. Clinical and molecular genetic analysis of a family with sitosterolemia and co-existing erythrocyte and platelet abnormalities. *Haematologica.* 2006;91(10):1392-1395.
36. Boesze-Battaglia K, Schimmel RJ. Collagen-stimulated unidirectional translocation of cholesterol in human platelet membranes. *J Exp Biol.* 1999;202(pt 4):453-460.
37. Maxfield FR, Tabas I. Role of cholesterol and lipid organization in disease. *Nature.* 2005;438(7068):612-621.
38. Kruit JK, Drayer AL, Bloks VW, et al. Plant sterols cause macrothrombocytopenia in a mouse model of sitosterolemia. *J Biol Chem.* 2008;283(10):6281-6287.
39. Rader D, Cohen J, Hobbs H. Monogenic hypercholesterolemia: new insights in pathogenesis and treatment. *J Clin Invest.* 2003;111(111):1795-1803.
40. Shultz LD, Lyons BL, Bronson RT, et al. Thrombocytopenia and cardiomyopathy (trac): a new single gene mutation resulting in severe platelet and heart abnormalities in mice. [abstract]. *Blood (ASH Annual Meeting Abstracts).* 2005;106:Abstract 734.